DESIGN AND EXPERIENCE WITH A 30,000 HP MAGNETIC BEARING SUPPORTED MOTOR DRIVEN TURBOCOMPRESSOR FOR A SPEED RANGE OF 600 TO 6300 RPM

by

Horst Kümmlee

Manager, Large Special Machines

Siemens AG

Berlin, Germany

Gerrit M. Lenderink

Manager, Compressor & Pump Engineering

Demag Delaval Turbomachinery B.V.

Hengelo, The Netherlands

Wim H. de Groot

Senior Rotating Equipment Engineer

Nederlandse Aardolie Maatschappij B.V.

Hoogezand, The Netherlands

and

Richard R. Shultz

Operations Manager

Federal Mogul Magnetic Bearings

Mystic, Connecticut

Horst Kümmlee is Head of the R&D Department for large rotating electrical machines in Siemens Dynamowerk, in Berlin, Germany. He is responsible for basic mechanical and electrical design, rotordynamics, simulation of electromechanical systems, measurement procedures and systems, and standardization. He has been at Dynamowerk since 1985 as Research Engineer, Head of the special machines order processing and design department, and in his current position.

Dr. Kümmlee graduated from the Technical University Berlin with a Dipl.Ing. degree (Mechanical Engineering, 1980), and received the degree of Dr.-Ing. for work on hyperelastic coupling elements and dampers (1985).

Gerrit M. Lenderink is Manager of Compressor & Pump Engineering for Demag Delaval Turbomachinery B.V., in Hengelo, The Netherlands. He joined Demag Delaval in 1979 and has more than 20 years of diversified experience in the fields of design, application engineering, and product development of centrifugal compressors. He has been heavily involved in the development of dry-dry compressors featuring dry gas seals and magnetic bearings.

Mr. Lenderink has a B.Sc. degree (Mechanical Engineering, 1979) from the Enschede Institute of Technology.

Wim H. de Groot is the Senior Rotating Equipment Engineer in the GLT project team of Nederlandse Aardolie Maatschappij B.V. (NAM), in Hoogezand, The Netherlands, where he serves as an advisor. Mr. de Groot was instrumental in the development of the functional specification and selection of the consortium members. He joined the NAM in 1971 and worked on several gas and oil field development projects.

Mr. de Groot has B.Sc. degrees (Mechanical Engineering, 1969; Contracts Engineering, 1971) from the Groningen Institute of Technology.

ABSTRACT

In the Northern Netherlands, after more than 30 years of production, the pressure of the gigantic Groningen onshore gas field is gradually decreasing, requiring up to 500 MW compression over the next 30 years to fulfil capacity obligations. Within a unique technical and contractual concept, up to 29 electric motor driven centrifugal compressors with 120 bar (1741 psi) discharge pressure will be installed to maintain the necessary input pressure for the Dutch pipeline network. Based on a thorough total cost of ownership evaluation, and considering the extended project duration and its special requirements, a future-oriented compression string was devised and installed in 1998, serving as the prototype for the remaining installations. Performance, design, and construction features of this oil-free turbocompressor string are described, highlighting the rotordynamic aspects of the supercritical rotating string with its extremely wide continuous operating speed range. The design aspects of the magnetic bearings

are emphasized. Test results and initial field experience are addressed. Lessons learned and a recommendation for the API Standards Committee conclude the paper.

INTRODUCTION

In 1959, Nederlandse Aardolie Maatschappij (NAM, hereinafter referred to as "the joint venture"), a 50/50 exploration and production joint venture of Shell and Esso, discovered large amounts of natural gas in the province of Groningen, in the northern part of The Netherlands. It turned out to be one of the largest gas reservoirs in the world. The production installations in the Groningen system consist of 29 standardized "well clusters," with a total of 300 wells. Groningen reserves have now dwindled to less than half the initially recoverable 2700 billion Nm^3, and the pressure in the field has declined from an original 345 bar (5004 psi) to about 145 bar (2103 psi) last year; free-flow capacity is thus rapidly decreasing. To maintain Groningen's vital function as a balancing producer, something had to be done to maintain the NAM's capability to produce the required annual volume while maintaining system capacity. The production capability can only be maintained by installing compression and by upgrading the clusters to the latest technology. In the first phase of an ongoing 15 year project, 11 clusters will each be equipped with a 23 MW electric motor driven centrifugal compressor. Fourteen more are envisioned to be equipped with about 12 MW each. The cluster at Tjuchem, near Slochteren where the field was discovered, was selected as the first benchmark cluster. Its compression string (Figure 1) has now been in operation for almost two years and it is the subject of this paper.

Figure 1. The Completely "Dry" Compression String at the Tjuchem Site of NAM in The Netherlands.

FUNCTIONAL REQUIREMENTS

Following a preselection of nine well known suppliers of large gas compressors, three consortia were invited to participate in a design competition. This competition was guided by a mere 47 page Functional Specification for the compression unit that challenged each consortium to come up with their best solution. It described in detail the expected operational usage of the compression unit over a 25 year period. It specified the scope of supply, the number of starts and stops, the annual load-factor, the desired operating envelope, the annual change in process conditions, references to API 617 (1995, bullet point paragraphs) and a Class III PTC-10 (1997) test. The document gave the manufacturers a maximum of freedom, with the objective to optimize their design to the lowest total cost of ownership (TCoO), often also called life- cycle cost (LCC).

Performance requirements are shown in Figure 2, which is an overall cluster well performance curve for the existing 11 wells of the Tjuchem cluster. It indicates the relationship between the flowing well head pressure and the total well production rates for particular reservoir pressures. Superimposed is the installation and transport line indicating the discharge pressure required to ensure the contractual 65 barg (943 psig) at the custody transfer stations to Gasunie, the operator of the Dutch gas transmission system. The iso-power lines indicate the correlation between flow rate and consumed power assuming a 78 percent compression efficiency. The area enclosed by the 7 MW and 23 MW iso-power lines reflects the expected operating area based on prestudies. This is the area that, as a minimum, had to be met. The desired operating area is enclosed by the 5 MW and the 30 MW iso-power lines. The remaining performance envelope between these areas and the discharge pressure line was expected to be covered by recycle on the compressor.

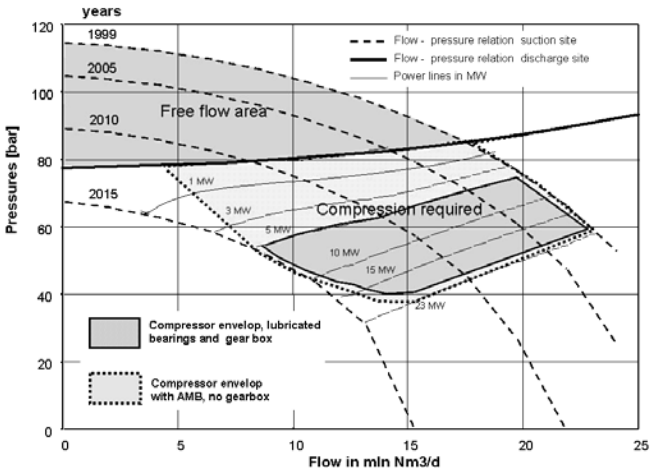

Figure 2. Performance Map as Basis for the Design Competition for the NAM GLT Project.

The gas delivery contracts of the joint venture require that a quick reaction to changing flow must be accommodated by the facilities. The pattern of morning and evening peaks must be followed by the clusters in operation. A startup period of 20 minutes for the compressor system in the cluster up to full flow was specified, plus a minimum of 500 start cycles per year, and three restarts in one hour. Startup reliability must be at least 99 percent and the compressor shall be able to remain pressurized during standstill for extended periods (months). Overall production availability (for the clusters in operation) shall be at least 96 percent and the availability of the compressor-driver unit itself, 98 percent during the winter. A no-failure-no-trip methodology must be applied in combination with a condition based maintenance philosophy.

The flat, agricultural landscape for the Groningen area requires that the new installations are blended into the existing clusters with minimum silhouette disturbance. There is, furthermore, a definite need to stay within the existing boundaries of the clusters. If this requirement is not met, additional land for each cluster would be needed, causing an elaborate acquisition and permit procedure with the various local authorities.

WHY ELECTRIC MOTORS?

An array of gas turbine options is readily available for the 23 MW range. So, why deviate from the traditional gas turbine driver

option and select an electric motor drive? The joint venture executed a detailed driver option evaluation taking into account:

- Reliability
- Performance
- Economics
- Emissions
- Site specific aspects

Reliability

The electric motor option introduces a dependency on the reliability of the power supply grid. Detailed studies indicated that the overall reliability would be at least as good as with the gas turbine option. Instrumental in this was the close proximity of a 1700 MW power plant and a high voltage power grid with various direct links to the Western European high voltage grid.

As far as the electric motor variable speed drives were concerned, the joint venture had very positive experience with even larger drives, indicating an overall significantly higher availability than comparable gas turbine drivers.

Performance

The present generation of gas turbines in the 23 MW range features a peak conversion efficiency on the order of 37 percent. However, by use of the present generation of large commercial combined cycle power stations to supply an electric drive, an overall conversion efficiency as high as 52 percent can be achieved. This includes all the transmission losses, i.e., natural gas to power at the compressor shaft.

The Groningen gas field is used as a peak flow supplier and is also the backup reservoir for all other gas fields in The Netherlands, in case they fail to supply. The annual load factor is therefore low (Figure 3). Most of the time (>90 percent), the field will run at loads below 50 percent. At these part load conditions, the conversion efficiency of gas turbines deteriorates to values as low as 25 percent and lower. However, the power plant feeding the electric drivers will maintain running on base load, i.e., conversion efficiency remains close to 52 percent. The net result is a significant conservation of valuable primary resources for the electric motor option.

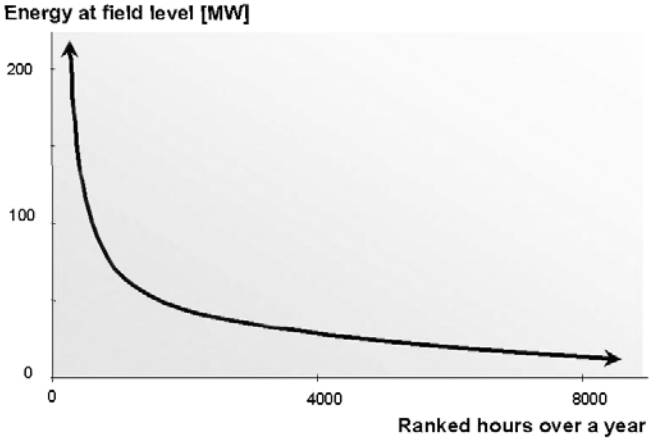

Figure 3. The Annual Load Factor of the Groningen Gas Field Is Very Low Due to its Mainly Peaking Service.

Economics

Purchasing decisions on plant equipment have traditionally been based on price. From a purely business point of view, procurement decisions should be based upon the total cost of ownership. The TCoO model applied to the Groningen project contains, but is not limited to, the complete investment costs (CAPEX), and the operational costs (OPEX) over a period of 25 years. The latter include costs of staff, energy consumption, emissions, and maintenance, including overhauls. The electric motor option came out significantly lower in terms of CAPEX. Instrumental in this case was the close proximity of a strong high voltage power grid.

At the time of the prestudies (1995/1996), the market for electricity in The Netherlands was deregulated and the readily available gas turbine option enabled the joint venture to negotiate an attractive contract with the local power supplier: the joint venture supplies natural gas to power stations and electricity is supplied to the joint venture in return. An energy conversion rate is charged to neutralize the energy component. The joint venture also pays a fee for the transport costs. With the energy savings included, as mentioned in the previous section, the cost difference in energy cost between the gas turbine and the electric motor option are virtually eliminated.

Emissions

The requirements on environmental issues in Holland are high. Although in the corresponding permits only the local emissions were mentioned, the joint venture also took into account in the driver selection study the related emissions of CO_2 and NOx of the power stations. Applied to the Groningen project, the overall emissions of the electric motor driven option came out significantly lower than for the gas turbine option (Figure 4). This was mainly due to the fact that continuous operation on base load inherently allows minimizing the CO_2 and NOx emissions. One could argue that a comparison between combined cycle and simple cycle by default would have this conclusion. However, the low load factor would not allow the joint venture to effectively apply the combined cycle principle for the gas turbine option.

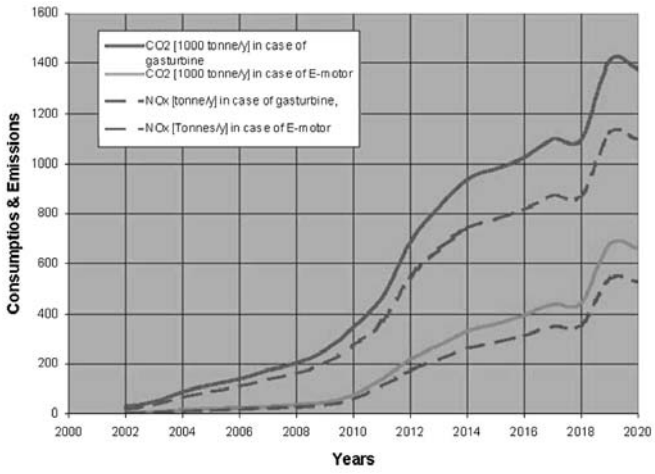

Figure 4. Total CO_2 and Nox Emissions Are Significantly Lower with Electric Drives.

Similar energy costs, at least as good reliability, and significant lower emissions pushed the selection toward the electric motor drive.

Site Specific Aspects

The noise requirements are stringent at these sites since they are located near populated areas. Due to their much smaller (cooling) air volumes and velocities, electric motors are inherently quieter than gas turbines, and keeping their sound pressure levels below 80 dB(A) is not a problem. However, in this project, most of the noise emissions were *not* coming from the compressor and its driver, but from the connecting pipelines, air-coolers (fans and motors), and pumps. Consequently, the turbocompressor-string could be installed outdoors on a flat concrete pad without the usual building—thus the required space for the compressor equipment

did not require an extension of real estate, which would have required an additional permit procedure.

A compressor enclosure would also affect the cluster silhouette negatively, which is important because the installations are located in a flat landscape. Also considering the safety point and explosion risks, installing the compressor at grade in the open air is preferred. There are no roofs or walls that will hinder access to the compressor during maintenance, which, if required, is performed on rainy days under temporarily installed tents. And finally, the omission of a building is also a major cost saving.

INTEGRATED DESIGN APPROACH

From the outset of the project, it was clear that the traditional procurement process would not yield the desired innovative compression system solution because new technology and much closer than usual client-vendor relationships were needed. Once the decision had been made to use magnetic rather than traditional oil bearings on the compression string, the manufacturers of compressor, motor, and magnetic bearings formed an alliance in the bidding period for the design competition and took an integrated design approach for the entire rotating string: the Stork GLT project consortium was formed that includes Demag Delaval (compressor), Siemens AG (motor, drive, and power supply), Federal Mogul (magnetic bearings), Yokogawa (I&C), Stork E&C, and a local construction company.

When properly designed, magnetic bearings offer fundamental advantages over traditional oil lubricated bearings—but their unique operating characteristics require more careful consideration at the design stage. Most notably, the rotational frequency dependency of the magnetic bearings, and their different specific load capacities, make their integration into the overall string design a more demanding process than the simple selection from standard ranges used for oil bearings.

There have been instances in early applications where magnetic bearings have been applied with the primary goal of removing the oil system, but thereafter their location and operation have been with the intent of making them look and behave like oil bearings. This approach led to a compromised design that neither capitalized on the many benefits of magnetic bearings nor fulfilled oil bearing expectations.

Within the Stork GLT consortium, the magnetic bearings were viewed as an enabling technology that is capable of delivering technical, operational, financial, and environmental benefits. As such, the integration of the magnetic bearings into the compressor and motor was treated as a primary component of the rotordynamic design. In particular, the design and location of the bearing components were an iterative process that was performed with the intent of optimizing the full motor/compressor string rotordynamic performance by the best arrangement of bearings, backup bearings, seals, and motor and compressor internals. A “traditional” layout would have resulted in suboptimal performance.

All the specified functional requirements ask for a very flexible, robust compression string with an extremely wide operating range. A closer look reveals that the differential pressure is proportional to flow squared, i.e., speed range is the key. The 15,000 actual m^3/hr (529,740 ft^3/hr) rated capacity and 130 barg (1886 psig) maximum working pressure promote the traditional application of a small size compressor with high shaft speed in combination with a step-up gearbox. But this solution is far from optimum:

- The majority of the cluster performance envelope remains uncovered and hence recycle is required.
- The large API 614 (1999) lube oil console associated with the gearbox makes it difficult to satisfy the cluster startup requirements and to install the compressor at essentially grade level.
- Integration of the compression equipment within the existing cluster plot plan is virtually impossible, and the resulting height of the installation would be a major blot on the landscape.
- Although well proven, the gearbox and associated components introduce additional complexity to the installation.

The TCoO-model clearly indicated that the gas turbine solution would not be satisfactory in this application mainly due to the energy savings related to omitting recycling in the prevailing part load operating mode. Therefore, the consortium focused on increasing the operating speed range preferably all the way down to standstill. It was then obvious that a more pragmatic, innovative approach was required, and the consortium decided to opt for an electric direct drive solution in combination with active magnetic bearings and dry gas seals (Figure 5).

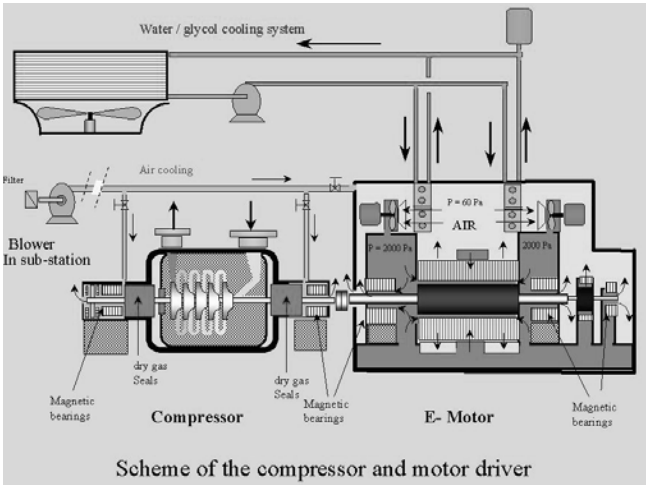

Figure 5. The Conceptual Arrangement of the Completely “Dry” Compression String Is Unique in the Industry.

Detailed analytical studies confirmed that operation down to zero speed would be feasible but not necessarily desirable, and control stability considerations within the drive system prohibited steady-state operation below 10 percent speed. The TCoO-model furthermore confirmed that one compressor revamp would be optimum.

COMPRESSOR DESIGN

Figure 6 is the initial five-stage configuration of the 55 ton fabricated compressor. The casing is supported by flexible legs thereby ensuring a true centerline support. This is essential given the extremely large operating envelope of this unit. The nozzles point upward enabling installation at grade. The bolted end head closure allows the arrangement of the majority of the auxiliaries at the compressor outer periphery, which enhances accessibility to the bearing bracket and simplifies maintenance.

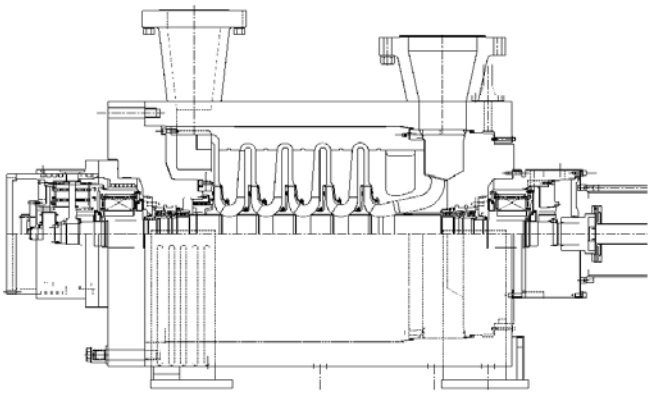

Figure 6. The Five-Stage Centrifugal Compressor with Magnetic Bearings Is Mounted at Grade Level.

The inner bundle, which can be withdrawn as one integral pullout pack with both end heads and bearing brackets, incorporates the five fully parametric compressor stages, the inlet section, and the discharge volute. The parametric concept allowed an optimum compromise between performance and rotordynamics. The applied abradable labyrinth geometry not only introduces some resilience during a nonlevitated rundown, but also ensures that the unit can be restarted following a nonlevitated rundown without overhaul. The rotor overall length is 3845 mm (152 inches), it weighs 2100 kg (4630 lb), and it is supported by two radial magnetic bearings. The large, double acting, axial magnetic bearing is arranged outboard at the nondrive end of the unit. Tandem dry gas seals in combination with segmented carbon ring barrier seals separate the bearing brackets from the impeller section.

A modular bearing bracket concept was adopted in order to minimize the need to dismantle parts. The magnetic bearings and backup bearings were installed in radial split brackets bolted directly to the casing. Special attention was given to the minimization of tolerance buildup and mechanical runout. The shaft sleeves for both magnetic bearings and the backup bearings were hydraulically mounted on the shaft.

MOTOR AND VARIABLE SPEED DRIVE DESIGN

Motor Design

As induction motors with suitable frequency converters are not on the market yet, the only electric motor applicable for the specified speed and power range is the two-pole brushless synchronous motor with a cylindrical, solid steel rotor. A brushless exciter is solidly coupled to the main rotor. It comprises an induction generator with a rotating rectifier wheel producing the DC power for the rotating motor field.

The solid steel turbo rotor is supported by three radial magnetic bearings, two at the motor section and one at the exciter section. The close to 5 m (5.5 yd) long rotor weighs 9300 kg (20,503 lb) and is essentially built out of two parts: the motor section and the exciter section. A single, high alloyed steel forging is used for the motor section with milled slots for the field winding, and the damper bars to withstand the centrifugal forces occurring at the maximum rotational speed. Nonmagnetic end caps and retaining wedges form the squirrel-cage damper winding that controls oscillating torques and harmonic currents in the rotor. Table I shows the rating data of the motor.

For each active magnetic bearing (AMB) a set of rotor sleeves is hydraulically shrunk onto the shafts (motor and exciter), each consisting of a laminated rotor sleeve assembly for the magnetic bearing, and a solid sleeve for the auxiliary bearing. This design ensures minimum mechanical runout and residual unbalance.

Along with a patented shaft design, the magnetic and backup bearings are arranged in a unique asymmetric way with respect to the motor/exciter stators. The AMBs on the drive end and exciter end are positioned outboard, while the AMB on the nondrive end is positioned inboard. This is the result of the rotordynamic analyses searching for the optimum compromise regarding the:

- Rotor behavior with the rotor being controlled by the active magnetic bearings under operating conditions.
- Rotor behavior with the rotor being supported by the backup bearings under emergency rundown conditions.
- Assembly of the bearings.

The preferred arrangement with respect to easiest assembly and maintenance of the backup bearings would have been an arrangement with the backup bearings being located outboard. However, this comprises rotordynamics.

The stator of the main motor is a welded housing structure with four ventilation circuits for symmetrical cooling and a very stiff laminated stator core. The two electrically offset stator windings are designed for Class F (155°C (311°F)) temperature rise, but they are only utilized to Class B (130°C (266°F)) in normal operation.

Table 1. Rating Data of High Speed Synchronous Motor.

Rated power & speed	23 000 kW @ 5400 rpm
Speed control range	600...6300 rpm
Constant power speed range	5400...6300 rpm
Rated voltage / current	2*3600 V / 2*2030A
Motor efficiency	98,0 %
Total motor weight / dimensions	70 t / 7m*3m*4,5m
Total rotor weight / length	9,3 t / 6,4m
Bearing span (main+exciter)	3,7m + 1,4m
Hazardous area classification	EExpII T3 (pressurized)

An air-water cooling system with four heat exchangers and four radial blowers is integrated into the motor enclosure creating an air flow of 13 m^3/sec (459 ft^3/sec) removing the maximum 460 kW of electrical and windage losses (Figure 7). Electric blowers for the inner cooling circuit were preferred over shaft mounted fans to reduce bearing span and to improve the cooling air distribution at low speeds. Even with failure of one fan or one cooler, the motor still can be operated at full power without exceeding the Class B temperature limit in the winding.

The drive system overall efficiency has been optimized taking into account the specific requirements of the Groningen application—it is still on the order of 70 percent when running at 10 percent speed. The motor is electrically optimized to a high torque-size ratio in order to minimize the bearing span. In addition, the flux versus speed profile is optimized, resulting in close to 98 percent motor efficiency over a wide speed range.

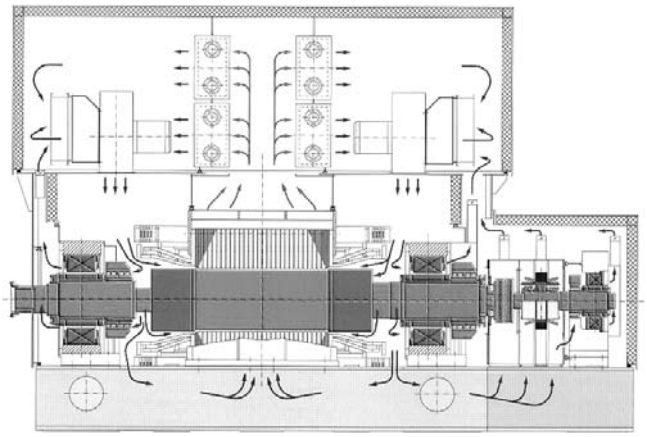

Figure 7. A Pressurized Enclosure Ensures Safety and Low Noise, and Symmetrical Cooling over the Entire Speed Range Is Ensured by Internal Radial Blowers.

Variable Speed Drive

The frequency converter (drive) applied to the Groningen project is a standardized and modular design that is used in hundreds of installations by several manufacturers: the specific model is of the simple load-commutated inverter (LCI) type in a parallel 12-pulse configuration, using high power thyristors as their solid state switching devices. In this type of drive, the motor itself controls the commutation of the converter thyristors (and thus its output frequency), and the motor current (which roughly equals torque since the flux in a synchronous motor is kept constant) is electronically controlled by varying the voltage in the DC link circuit.

The construction of the Megawatt size LCI converters is modular. The heat producing components are water cooled by means of a closed loop deionized water circuit. The DC link reactors are also directly water cooled and integrated into the drive enclosure, simplifying its installation and reducing footprint and costs at the same time. To accommodate the client's requirements for comprehensive type and performance tests prior to the jobsite installation, all major subsystems were constructed as

prefabricated modules on skids that were then installed inside the site erected buildings. Buildings were required for architectural reasons in this case.

Nonlinear electric loads, such as these frequency converters, produce harmonic currents that cause voltage distortions in the feeding power system, and they have a poor power factor at part load and speed. These effects are minded by the utility company since they can substantially disturb other consumers and make power transmission inefficient. Based upon a comprehensive network analysis, special circuit configurations and custom tailored harmonic filters were selected, reducing the distortions to acceptable levels.

Magnetic Bearings

The radial magnetic bearings, of which there are two in the compressor and three in the motor (Figure 8), are of the heteropolar design with two orthogonal axes of control per bearing. The radial bearing axes of control are oriented at 45 degrees from the horizontal. Silicon steel is used for the rotor and stator laminations. The rotor sleeves are located with a taper fit since the sleeves on the compressor must be removed to perform maintenance on the dry gas seals.

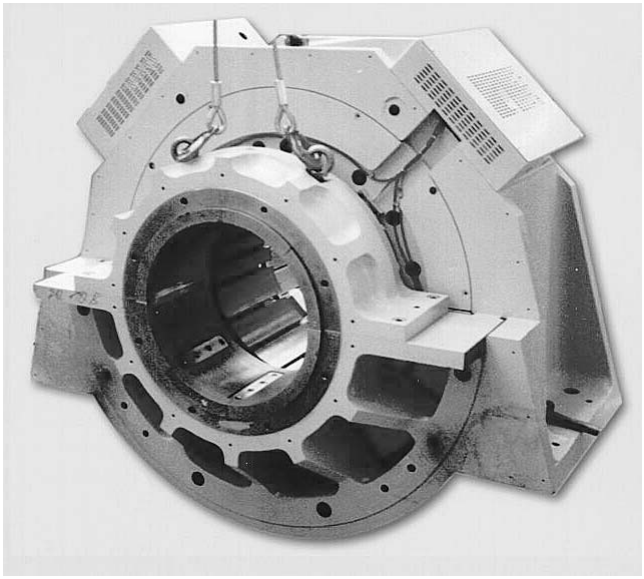

Figure 8. An Active Magnetic Bearing Design with Levitation (Rear) and Static Mechanical Backup (Front) Fully Controls the 9300 Kg Motor Rotor.

The axial bearing in the compressor is a double acting three-pole "E2" type design. Its axial collar is made of a conventional solid material and the stators are fully laminated to yield enhanced damping and control in the axial dimension.

The winding insulation on both the radial and axial magnetic bearings is rated to 180°C (356°F). Control of the rotor is based upon position and velocity feedback sensors, which are collocated, on common sensor modules. Each radial bearing has sensors at both the inboard and outboard end of the lamination stacks, and the sensor type is magnetic to allow direct shaft sensing. This is important to maintain a stable reference to the inertial axis of the rotor and thereby avoid the introduction of geometric runout when the compressor lamination sleeves are removed for seal accessibility.

Backup Bearings

The radial and axial backup bearings are of a dry bushing rotor delevitation system (RDS) design. The radial bearings use an articulated pad design, allowing the pads to align to the landing sleeve and to provide an adjustable compliant mounting. The stiffness and damping coefficients of the mounts are tuned to control the dynamic loads and vibration amplitudes during a landing event. In the motor, the backup bearings are split for ease of assembly and maintenance.

The condition of the shaft bushings is observable from the control cabinet after a delevitation by adjusting rotor position during static levitation to assess clearance degradation. This feature allows a determination of remaining backup bearing life, without machine disassembly, since wear is the only indicated failure mechanism of the bushing material. The dry bushing is also tolerant to any contamination that may build up during the operating life of the compressor while the backup bearings are not in use.

During emergency situations—which result from the complete loss of the uninterruptible power system (UPS) supplied AMB power and control electronic system—the spinning rotor will drop onto the backup bearings and is braked to standstill by the resulting friction. To significantly extend the service life of the backup bearings, the variable speed drive system (VSDS) control will—once it receives a fault message from the AMB control system—electrically brake down the rotating string from maximum speed to zero within five to 10 seconds—with the help of the compressor load. In reality, AMB amplifier, control system, and power supply failures are an extremely rare event. Due to the separately backed up power source of the AMB-system, a simultaneous power loss of VSDS and AMB-control is even more unlikely.

Bearing Control System

The magnetic bearings for both the motor and compressor are controlled by a single combined system. The digital controller utilizes a rugged virtual machine environment (VME) system to calculate a complex eighteenth order polynomial for each axis of control to produce the overall bearing transfer function. The power amplifiers for each bearing axis are rated at 15 kVA in the compressor and 30 kVA in the motor.

Magnetic bearings have well defined dynamic load capacity limits determined by the kVA rating of the power amplifiers and the magnetic actuator load capacity and inductance. The dynamic load capacities for the motor and exciter magnetic bearings are shown in Figure 9.

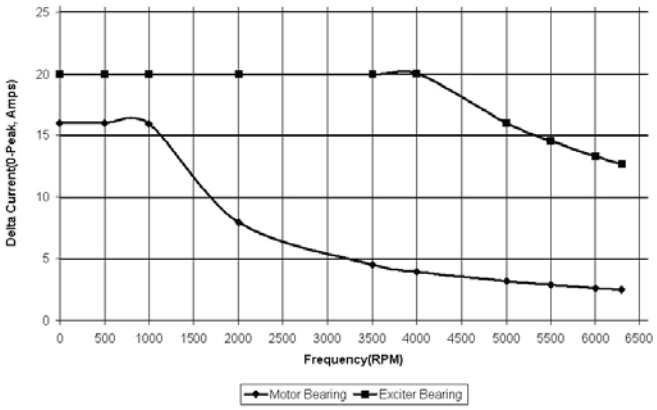

Figure 9. The Dynamic Load Capacity of the Mag-Bearings Is Matched to the Specific Operating Conditions.

The approximate conversion to dynamic force (zero-peak) is 572 lb/amp for the motor bearing and 120 lb/amp for the exciter bearing. The dynamic load limits are defined here as the dynamic magnetic bearing current. Defining the limits with dynamic current is of great practical use, since the currents are normally monitored

by the magnetic bearing system and actual bearing force measurement is not readily available.

An optimum level of redundancy is designed into the system: the input power feed is dual redundant battery backed to allow up to four hours of autonomous operation. All other critical power supplies within the cabinet are either n+1 or n+2 redundant. The motor bearings are wound with dual coils and use dual amplifiers per axis. Minor maintenance items, such as cooling fans, are hot swappable during dynamic operation.

Remote monitoring and diagnostics of all bearing system parameters are performed via a modem link to the central control cabinet, following the transmission control protocol/Internet protocol (TCP/IP). The prime diagnostic information sources within the system are the event logs and the trip data. The event logs allow the sequence of events to be recorded. The trip datum is a continuously updating 30 second burst of sample rate data containing information on all position and current signals. These data can be used for remote visualization using "standard" displays like waterfall plots or polar diagrams.

ROTORDYNAMICS

Lateral Rotordynamics

A close to 11 m (12 yd) long compression string weighing 11,400 kg (25,132 lb), supported by five radial magnetic bearings, and a speed range from 10 percent to 105 percent is unique in the industry. The motor is furthermore the first of its kind in the industry. The goals for optimizing a rotor design with magnetic bearings are to satisfy vibration amplitude and amplification factor requirements with a minimum amount of bearing damping and to minimize the dynamic bearing loads for a given amount of unbalance. Specifying API vibration criteria, however, is not optimum as this would mandate high stiffness and damping from the active magnetic bearing system with inherent high dynamic currents. This would make the control loop overly sensitive and result in an inherent risk of saturation of the power amplifiers at even small disturbances.

The applied vibration criteria were therefore derived from the following parameters:

1. No contact with bearings, adjacent displacement sensors, and backup bearings

2. Limiting dynamic current in relation to power amplifier capacity

3. Based on operating experience, a minimum logarithmic decrement criterion was set at 1.0. (Dynamic amplification factor not exceeding 3.2 within the operating speed range.)

The lateral compliance of the applied 900 mm (36 inch) DBSE contoured diaphragm string coupling provides effective dynamic decoupling between the motor and the compressor, which allowed the independent optimization of both units.

MOTOR ROTORDYNAMICS

High speed synchronous motor rotors typically have high slenderness ratios due to necessary design features. Traditionally, high speed synchronous motors have been operated with oil bearings. The same general rotor design guidelines used for the oil bearing design were adhered to for the magnetic bearing machine. Since the motor is operated continuously anywhere within the speed range, adequate stability margins are required for continuous operation at the bending modes.

Open Loop Behavior

Figure 10 is the undamped critical speed map of the motor. The map includes the zero speed and the forward and backward modes at maximum running speed since all these modes must be stabilized by the magnetic bearing system.

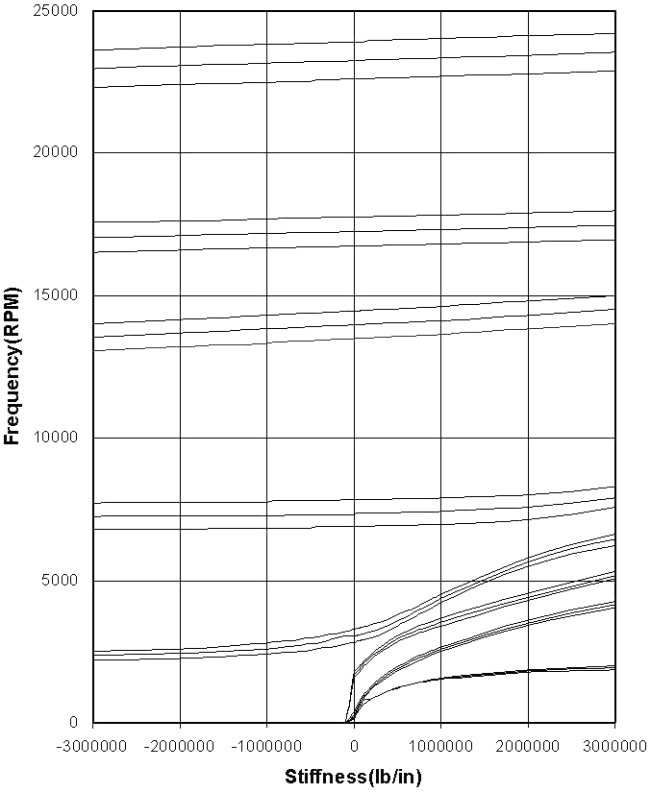

Figure 10. The Undamped Critical Speed Map of Motor.

Figure 11 shows the related mode shapes of the complete motor rotor with a bearing stiffness of 300,000 lb/in and exciter bearing stiffness of 80,000 lb/in. Many design iterations were studied to optimize the rotor design.

Figure 12 shows two different configurations considered during the design process. Design "A" has both motor magnetic bearings located outboard of the auxiliary bearings, and the motor stub shaft diameters are symmetric on each side of the motor core. For Design "B," an asymmetric bearing arrangement was applied in combination with a reduced shaft diameter at one side of the motor core. Design "B" offers increased rotor flexibility through more shaft motion at the drive end bearing for the first bending mode, making the bearing more effective for damping the mode. Therefore Design "B" was chosen as the final design. Other key design features of the final design are: the nondrive end motor magnetic bearing is located inboard of the auxiliary bearing to minimize the dynamic bearing load at maximum running speed, and the exciter magnetic bearing is located outboard of the auxiliary bearing to make the best use of the available bearing damping.

Closed Loop Behavior

The complete magnetic bearing/rotor system stability is evaluated with a complex eigenvalue analysis. Frequency domain characterizations of all magnetic bearing system components including sensors, controller, amplifiers, and actuators are combined with the rotor characteristics for this analysis. Table 2 is a listing of the system complex eigenvalues for the zero speed and the maximum running speed cases. As previously mentioned, all modes within the operating speed range have a logarithmic decrement of approximately one or greater. For modes with frequencies higher than the maximum running speed, operational experience with other magnetic bearing systems has demonstrated satisfactory operation with small positive logarithmic decrements.

For machines with flexible rotors running in magnetic bearings, it is important to specify the expected worst case imbalance distributions. Figure 13 shows that for 20 oz*in of coupling

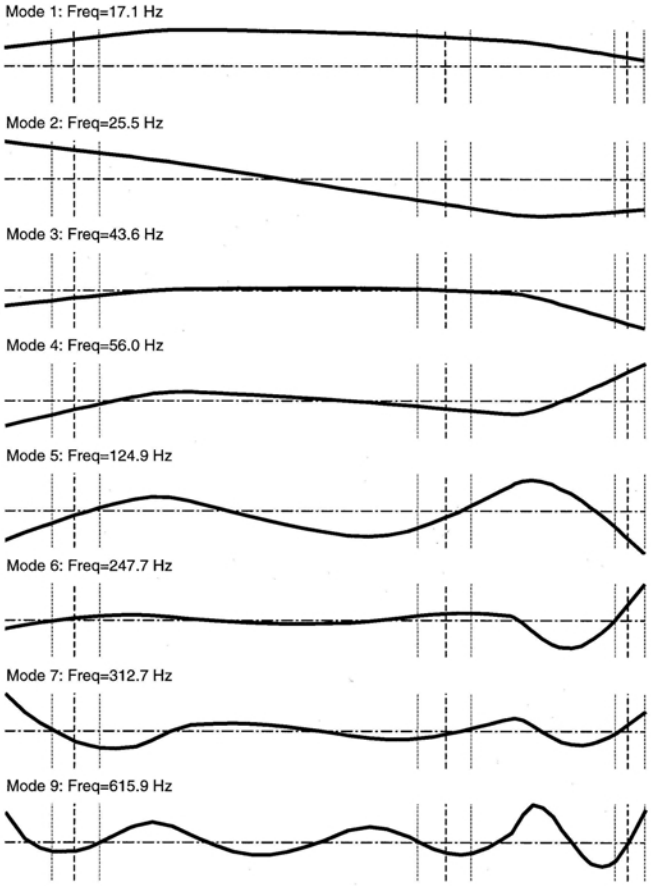

Figure 11. Mode Shapes of the Complete Motor Rotor.

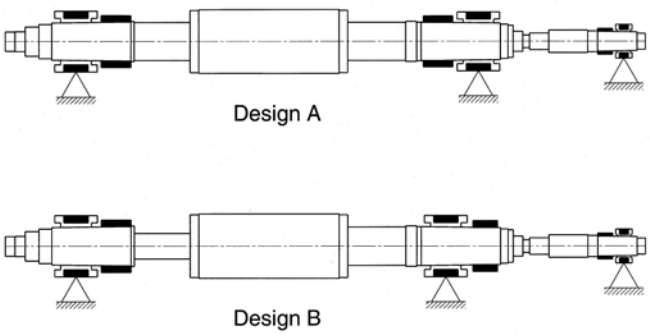

Figure 12. Two Types of Rotor Bearing Designs Were Studied; Design "B" Was Finally Chosen.

imbalance, the drive end bearing comes close to the dynamic limit of 2.5 amps. An imbalance of 20 oz-in applied anywhere else on the rotor results in much lower dynamic currents.

COMPRESSOR ROTORDYNAMICS

Because of the numerous design tradeoffs in the compressor design, opportunities were limited for optimizing the rotor design for the magnetic bearings: minimum low frequency damping requirement, minimum damping requirement at rigid body and bending modes, strong seal effects, large operating speed range, and small inherent shaft damping. The bearing stiffness also must be high enough to resist fluid forces both DC and AC in nature.

Open Loop Behavior

Figure 14 shows the calculated undamped critical speed map of the compressor.

Table 2. System Complex Eigenvalues Motor.

Rotational Speed	0 RPM		6300 RPM	
Mode Description	Frequency (RPM)	Log. Dec.	Frequency (RPM) Backward Forward	Log. Dec.
Translation	1014	1.78	1013 1015	1.75 1.80
Tilting	1460	2.63	1395 1525	2.63 2.62
Rotor First Flexible	2470	1.95	2373 2571	1.96 1.94
Rotor Second Flexible	3301	0.96	3081 3535	0.99 0.93
Controller Pole	5130	1.94	5129 5147	2.00 1.96
Rotor Third Flexible	7548	0.01	7070 8061	0.01 0.01
Rotor Fourth Flexible	14967	0.01	14.382 15.557	0.01 0.01
Rotor Fifth Flexible	18801	0.01	18.195 19.415	0.01 0.01
Controller Pole	33000	0.94	33.000 33.000	0.93 0.95

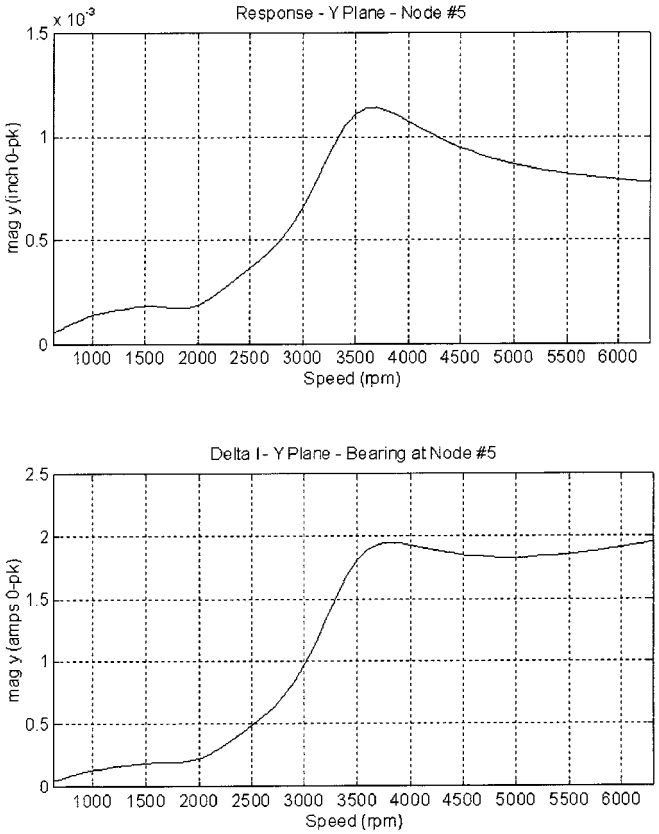

Figure 13. Unbalance Response at Main Coupling.

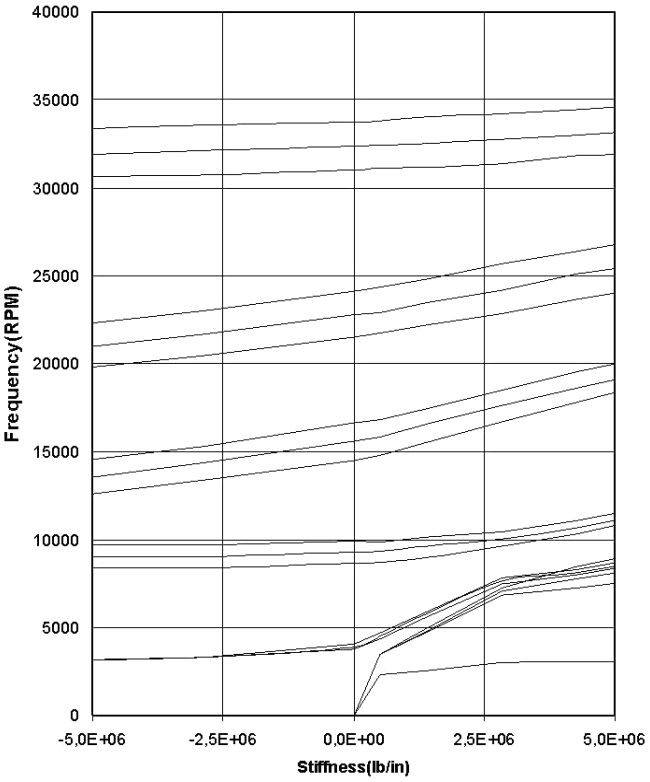

Figure 14. The Undamped Critical Speed Map of the Compressor.

Table 3 lists the location of the natural frequencies for different bearing stiffness both at standstill and at maximum continuous speed. The shift in natural frequency between standstill and full running speed indicates that the rotor has a gyroscopic effect that is caused by the large diameter impellers and thrust disk, which have all been modeled as rigid connected masses with polar and transverse inertia.

Table 3. System Complex Eigenvalues Compressor.

Rotational Speed	0 RPM		6300 RPM	
Mode Description	Frequency (RPM)	Log. Dec.	Frequency (RPM) Backward Forward	Log. Dec.
Translation	850	1.66	847 853	1.66 1.66
Tilting	944	1.78	930 958	1.78 1.78
Controller Pole	2148	1.12	2142 2154	1.10 1.14
Rotor 1st Flexible	4870	1.05	4639 5082	1.08 1.01
Controller Pole	7788	0.39	7728 7848	0.43 0.35
Controller Pole	7811	0.55	7751 7871	0.48 0.62
Rotor 2nd Flexible	9206	0.07	9596 9816	0.08 0.06
Rotor 3rd Flexible	14960	0.01	13520 16400	0.01 0.01
Rotor 4th Flexible	21180	0.01	18900 23460	0.01 0.01

Figure 15 shows the associated rotor mode shapes at standstill. All mode shapes of interest have acceptable controllability (amplitude at the bearing actuator position) and observability (amplitude at the sensor position).

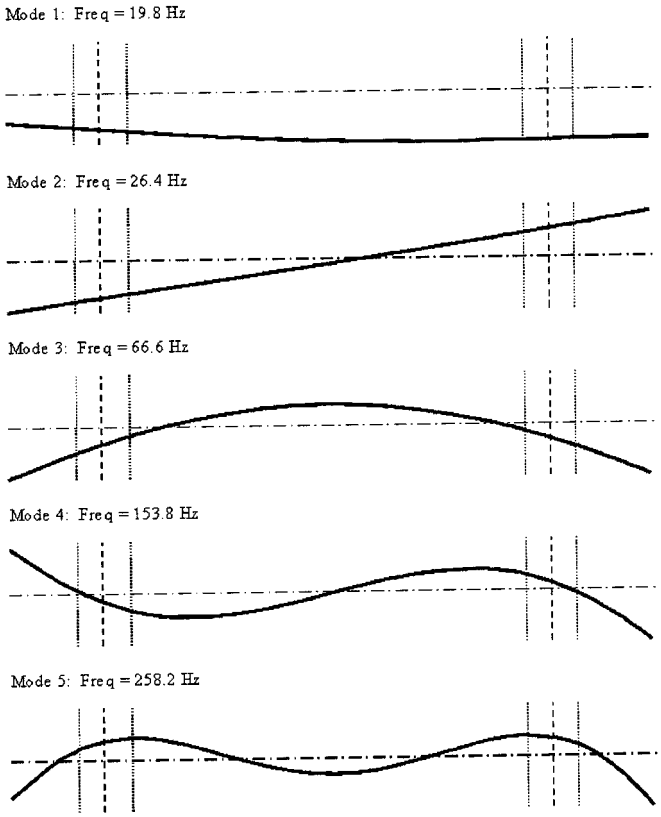

Figure 15. Undamped Mode Shapes of Compressor Rotor at Standstill Indicate Controllability and Observability.

The eigenvalues (natural frequencies and damping ratio) of the combined rotor bearing system at nominal speed and standstill are listed in Table 3. All modes below maximum continuous speed are well damped. The first bending mode has a logarithmic decrement close to 1.0 (damping ratio D = 17.3 percent), which is close to the API 617 (1995) requirement. All modes below 800 Hz are stable. Above 800 Hz instability may occur, since the phase angle of the bearing then becomes negative. In reality, the internal damping of the rotor will most probably prevent these instabilities, since the negative damping has a very small magnitude.

The closed loop response to an unbalance modal excitation for the various critical speeds of interest has been evaluated. The response is well damped throughout the operating speed range from 600 to 6300 rpm. The maximum bearing forces are well within the 2250 lb dynamic bearing capacity at 105 Hz.

Table 4 is the result of the stability analysis taking into account full aerodynamic excitation. It can be seen that stable operation is predicted throughout the operating speed range.

Torsional Rotordynamics

The rotor train must be designed to withstand the torque amplifications for startup, normal operation, and also for fault conditions. The main torsional excitation for the train is generated by the current harmonics of the 12-pulse converter fed motor. Therefore it is necessary to choose a rotor design where the relative deflection in the area of the rotor is low for the significant mode shapes.

Figure 16 shows the calculated undamped torsional critical speed mode shapes of the compressor string.

Table 4. Stability Analysis of Compressor with Full Aerodynamic Excitation.

Rotational Speed	6300 RPM Without Seal Effects		6300 RPM With Seal Effects	
Mode Description	Frequency (rpm) Backward Forward	Log. Dec.	Frequency (rpm) Backward Forward	Log. Dec.
Translation	847 853	1.66 1.66	552 1152	6.38 0.31
Tilting	930 958	1.78 1.78	737 1024	4.36 0.67
Rotor First Flexible	4639 5082	1.08 1.01	4716 5032	0.99 0.94

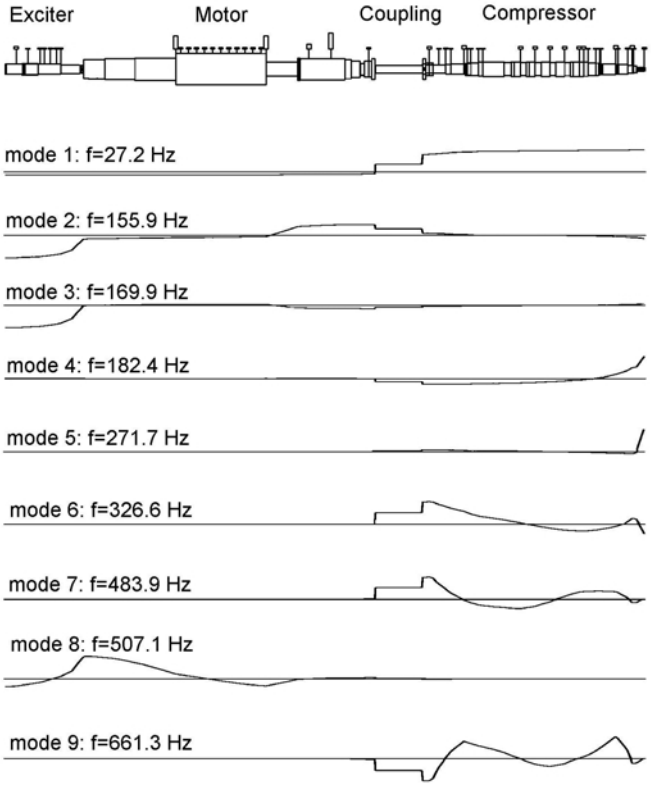

Figure 16. Undamped Torsional Critical Speed Mode Shapes of the Compressor String.

The Campbell diagram (Figure 17) shows possible points of resonance condition for steady-state operation.

Despite the direct drive configuration, it is technically not feasible to remove all criticals from within the extremely wide operating speed range. The design of the rotor string (motor, coupling, and compressor) is governed mainly by performance and the lateral behavior of the individual string components. The first torsional critical speed can be adjusted by selective tuning of the coupling.

Stationary Resonance Analysis

All air gap pulsating torques appear in the center section of the motor. Figure 18 shows the system response in coupling and exciter shaft due to an exciting torque of 1000 Nm at the center of the rotor core and 1 percent critical damping. The stresses are represented in the coupling spacer and in the exciter coupling shaft as N/mm^2.

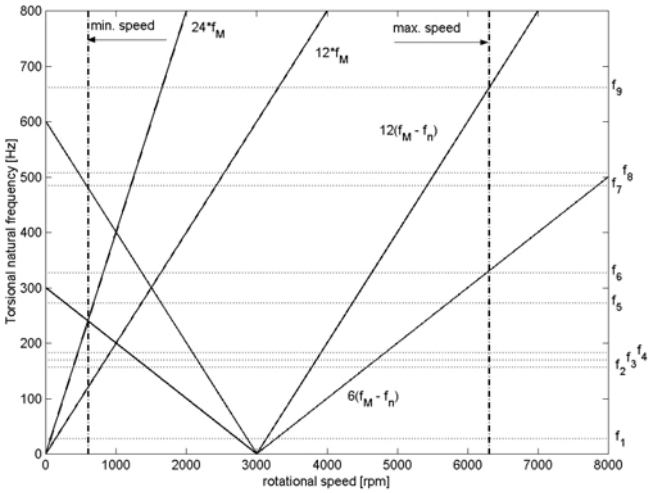

Figure 17. Campbell Diagram with Possible Points of Resonance Condition for Steady-State Operation.

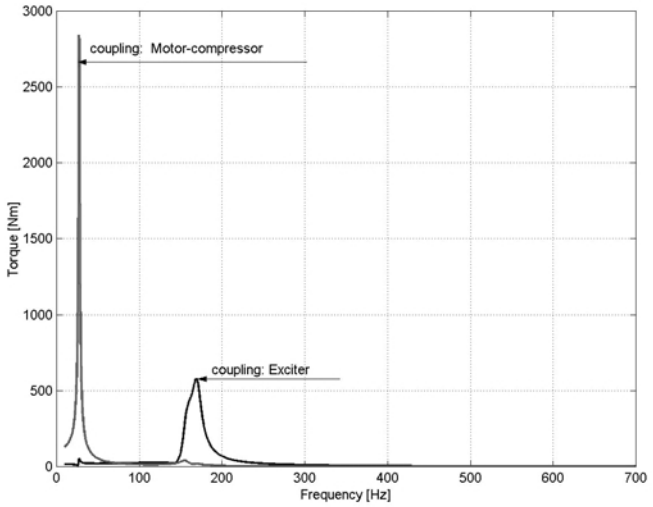

Figure 18. Torque Response Due to Steady-State Excitation with 1000 Nm at Midspan of Motor Core.

It can be recognized that the first resonance peak dominates the behavior and represents the maximum stress amplification in the string. A detailed fatigue analysis confirmed that the calculated stresses are acceptable and continuous operation would be possible. All further resonances have relatively low amplifications and can be neglected.

Startup Analysis

During the startup process, various torsional natural frequencies are passed. Only the first one brings significantly higher stress in some sections of the shaft system: In the speed range 2600 rpm ≤ n ≤ 3400 rpm, the first natural frequency is excited four times (Figure 17). The result of a startup simulation is shown in Figure 19.

Fault Condition Analysis

The main electrical fault conditions are:

- Three-phase short circuit at the motor terminals

$$M(t) = 9.8 \cdot M_N \cdot e^{\frac{-t}{0.182}} \cdot \sin(660 \cdot n \cdot t) \quad (1)$$

- Line-to-line short circuit at the motor terminals

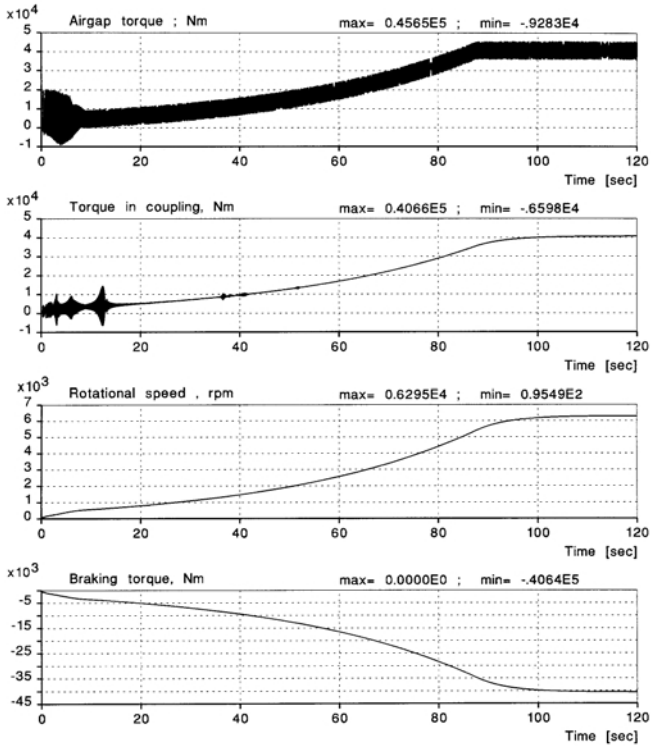

Figure 19. Runup Through Resonance with Nominal Torque Poses No Danger to the Rotating String.

$$M(t) = 9.8 \cdot M_N \cdot \left[\frac{e^{\frac{-t}{0.097}\frac{-t}{0.306}} \cdot \sin(660 \cdot n \cdot t)}{-0.5 \cdot e^{\frac{-2 \cdot t}{0.306}} \cdot \sin(2 \cdot 660 \cdot n \cdot t)} \right] \quad (2)$$

where n is the actual rotating speed divided by the reference speed n_N = 6300 rpm.

It can be seen that the frequency of the short circuit excitation is a function of the actual motor speed. The worst condition is when the excitation frequency coincides with one of the natural frequencies of the drive train, whereby the most critical torsional modes are the first and the second one where the motor shaft has a certain amplitude at the motor core. The calculated short circuit response is shown in Figures 20 and 21. In looking at these fault scenarios, however, one has to consider the extreme unlikeliness of such an event in actual installations. Nevertheless, precautions in the form of controlled-slip fits and shear points are installed to mitigate this risk.

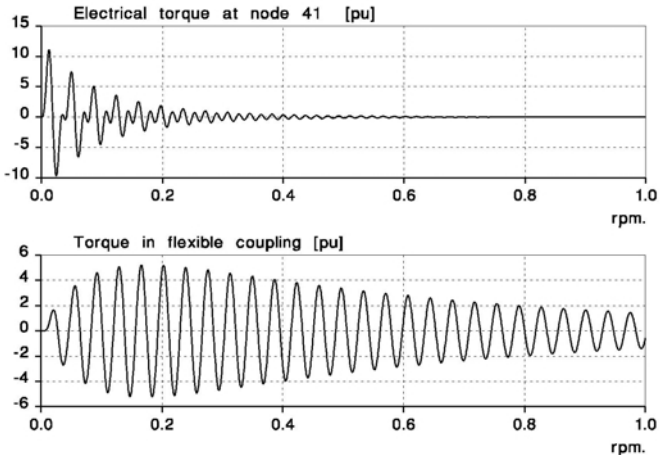

Figure 20. Two-Phase Short Circuit at 1530 RPM.

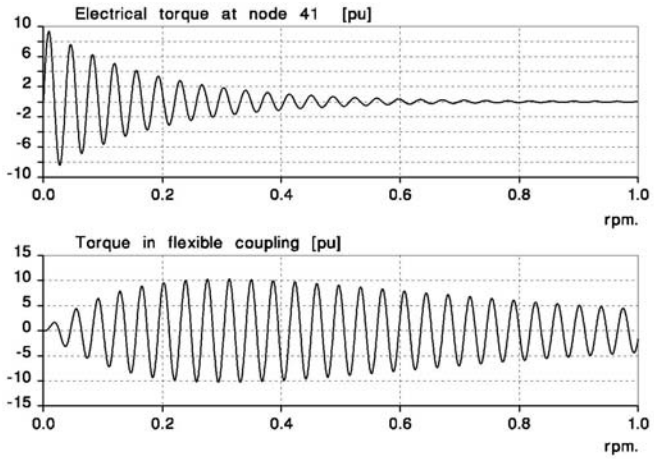

Figure 21. Three-Phase Short Circuit at 1530 RPM.

The detailed damped response calculations, both steady-state and transient, confirmed that continuous operation over the extreme wide operation range from 600 to 6300 rpm is feasible. Beneficial in this respect was the inertia split of the large synchronous motor and the compressor.

The calculated stress levels were all well within the acceptance limit.

TESTING

Motor

Basic motor rotordynamics were established through modal analysis with the rotor supported vertically from a crane. Static tuning of the assembled motor rotor was done followed by high speed balancing of the motor rotor in its magnetic bearings.

Various balancing planes enable a modal balancing of the finished rotor. The motor rotor was not high speed balanced on a balance stand, but directly in its magnetic bearings since all balancing planes were readily accessible. This was followed by unbalance response sensitivity checks indicating that the motor responded very well.

Field experience on this class of electric motors indicates that, once balanced, deterioration of the balance quality is not anticipated. However, different from a centrifugal compressor, the motor rotor must handle electromagnetic pull from both the exciter and main motor stator section, as well as thermal gradients during startup and changing operating conditions. This introduces significant dynamic loads that have to be taken into account. An extensive test program was set up to verify the integrity of the design. The applied concept of separate base frames for motor and compressor, the lateral compliance of the interconnecting coupling, and dedicated magnetic bearing controllers allowed simultaneous execution of this test program at both the compressor and the motor supplier's works.

The sensitivity to imbalance for the motor rotor/bearing system was measured over the running speed range. Figures 22, 23, and 24 show the comparison between the measured values and the calculated values for the imbalance case of 20 oz*in applied out-of-phase at each rotor core end cap. The calculated values are in good agreement with the measured values.

Static and dynamic tuning were completed in a straightforward manner with no problems. This was attributed to the optimized motor rotor design, the significant internal damping inherent with these types of rotors, and use of the experiences related to the control system software gained at the compressor supplier works.

Compressor

The compressor rotor was high speed balanced in oil bearings. Dedicated shaft sleeves replaced the contract laminated sleeves for

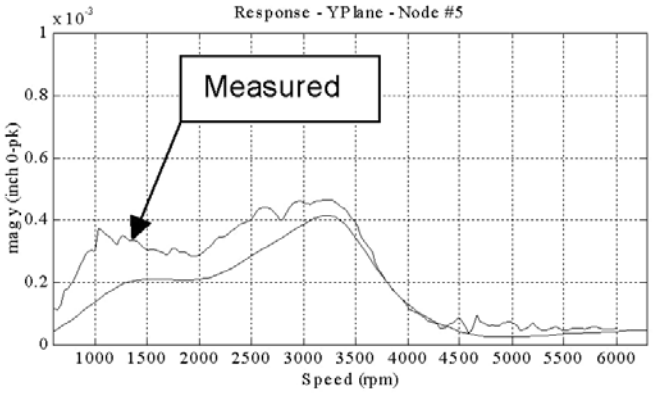

Figure 22. Drive End Bearing—Unbalance Response Out-of-Phase at Motor Core End Caps.

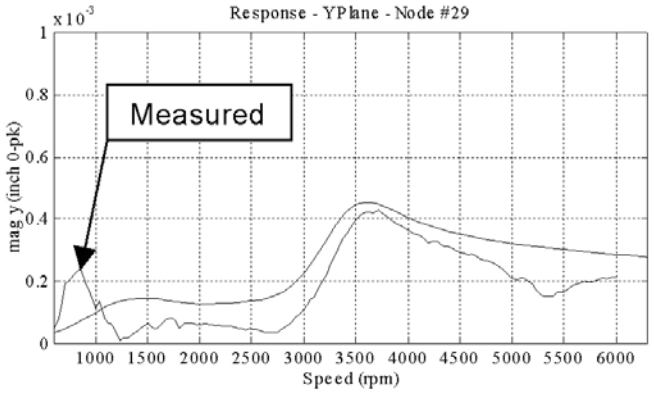

Figure 23. Non Drive End Bearing—Unbalance Response Out-of-Phase at Motor Core End Caps.

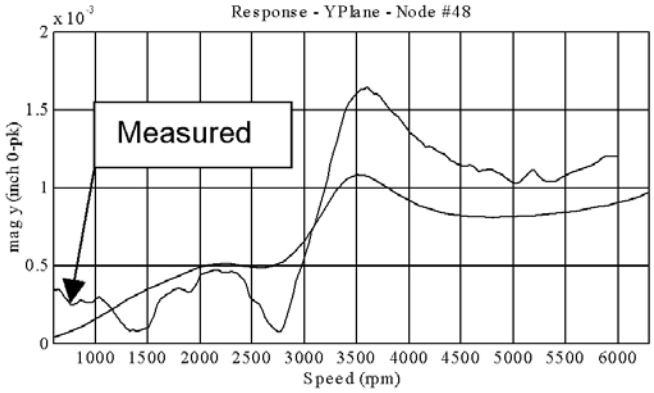

Figure 24. Exciter Bearing—Unbalance Response Out-of-Phase at Motor Core End Caps.

this purpose. The basic rotordynamics were verified using modal analysis with the rotor supported horizontally in slings. Static tuning of the assembled compressor was done with the dry gas seals and labyrinths removed. Soon it became evident that the targeted magnetic bearing control strategy would not be adequate for this unit. A high frequency mode at 490 Hz interfered with the roll-off region of the controller. Interim high order filters were tried but none were successful. It was concluded that more testing would be required to get a better understanding of what was going on. The rotor was sent back to the balancing bunker and the disk behavior was recorded during a full operating speed range run under vacuum. It became evident that the disk had several disk modes within the frequency range of interest caused by its slender nature design. Detailed analytical checks using FEA confirmed that the disk had a nodal diameter vibration mode at approximately 490 Hz, which had to be considered in the rotor model (Figure 25).

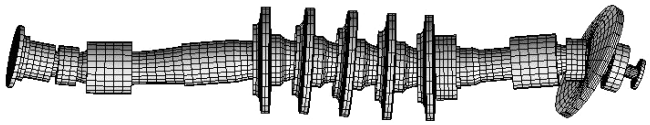

Figure 25. FEA Compressor Mode Shape at 490 Hz.

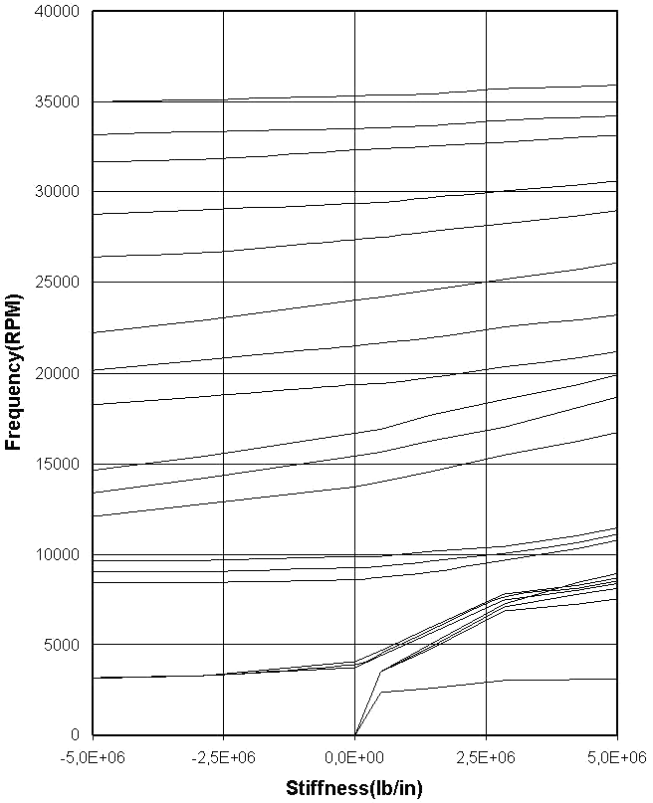

Figure 26. Revised Undamped Critical Speed Map of Compressor with Compressor Disk Fixed to the Rotor by a Rotational Spring to Meet the 490 Hz.

To model this mode, the disk was fixed to the rotor with a rotational spring. The stiffness of this spring was adjusted to yield the 490 Hz. The results are plotted in Figure 26.

It can be seen that the disk mode and the rotor modes are interacting. In the second and higher bending modes, the flexible disk tilts more than a rigid disk would. This has the effect of considerably increasing the gyroscopic effect. As a consequence, the frequency difference between forward and backward whirl also increases and thus the frequency regions where the bearing has to provide damping. This explained why the initial control strategy did not work out as predicted. A revised control strategy was selected and implemented, and static tuning was completed successfully before the unit was prepared for dynamic testing.

The compressor was admitted to an unbalance sensitivity test. Unbalance weights were placed at both the thrust disk and the coupling location. Bearing response to an in-phase G2 unbalance (3300 g (117 oz) at the thrust disk, and 2700 g (95 oz) at the coupling) is shown in Figure 27.

It can be seen that the measured response is in good agreement with the prediction and furthermore that the absolute magnitude is well within the bearing load capacity. To mimic a dry gas seal maintenance cycle, the magnetic bearing components were disassembled and then reassembled. The response was checked and it matched the original.

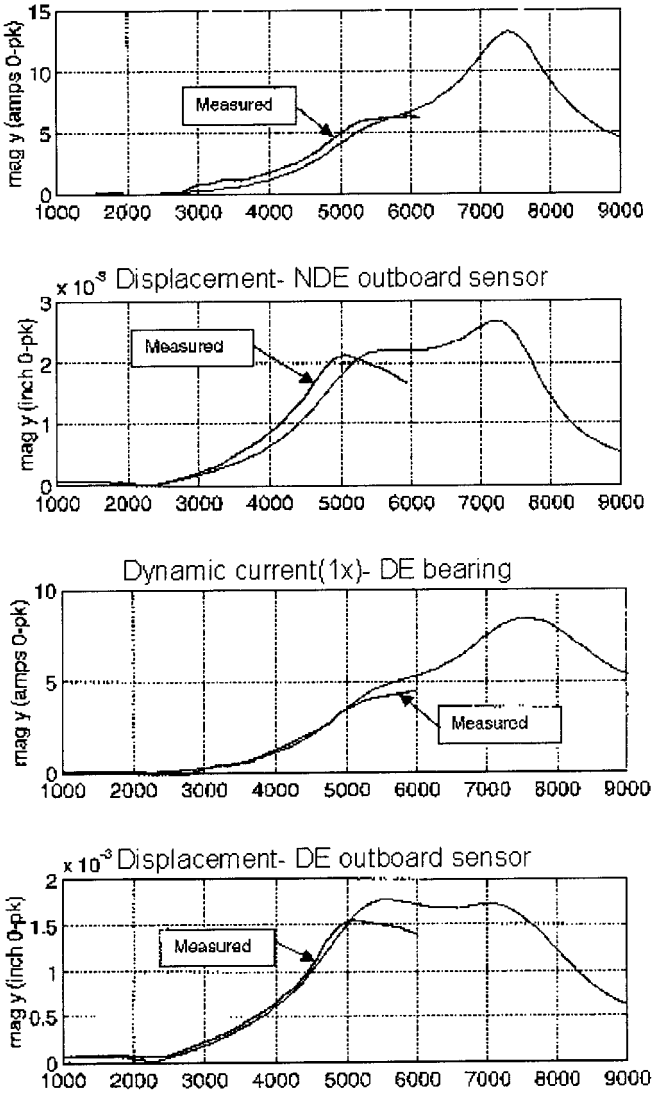

Figure 27. Unbalance Response Test of the Compressor.

A 12 MW, part load, full speed hydrocarbon test was one of several executed. The inhouse high pressure natural gas grid connection at the supplier's works allowed the use of basically Class I conditions. Test results are shown in Figure 28 and it can be seen that an excellent match is yielded compared to the prediction. During these tests, the magnetic bearing control system recorded low frequency, forced vibrations when operating the unit under turndown conditions at high speed. Dynamic pressure pulsation measurements cohered well with these recordings, confirming that these vibrations were forced by aerodynamic excitation most likely caused by off-design operation at these high speeds. However, the magnitude of the pressure pulsation was only in the mbar region. The recorded sensitivity was explained by the lower stiffness of the magnetic bearings compared to oil bearings at these low frequencies.

During testing, the rotor was subjected to a nonlevitated rundown from full speed down to approximately 3000 rpm.

Following this test, the backup bearings were checked and found in excellent condition. Some material transfer from the stator pad lining to the sleeve on the rotor was observed, which is inherent with the design used here. During this test, a high dynamic load was imposed on the rotor that was believed to simulate an extreme unbalanced rundown situation. The observations and measurements afterward confirmed that the landing system was fit for purpose.

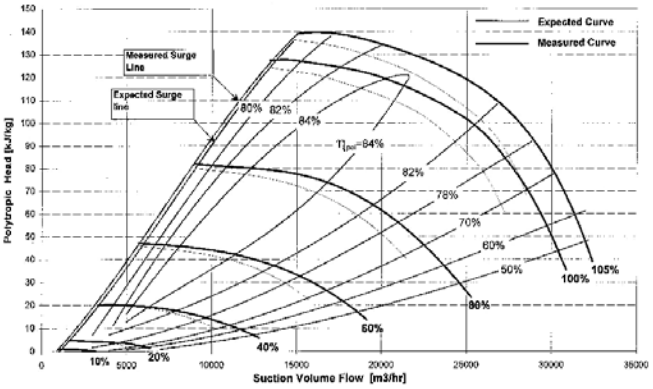

Figure 28. Full Speed, Part Load (12 MW) Hydrocarbon Test of Compressor.

FIELD EXPERIENCE

The equipment was shipped to site in the summer of 1998 and hooked up to the cluster. The motor was initially run solo. Everything proved satisfactory and the interconnecting coupling was installed. The axial magnetic bearing controller was tested for the first time with the motor and compressor joined by the high axial stiffness coupling. Axial dynamic testing to verify satisfactory performance of the axial bearing controller was completed in a day, and the unit was run to full speed using nitrogen. As expected, the lateral compliance of the coupling provided sufficient dynamic isolation between the two machines so no changes were required in the radial bearing algorithms. All parameters proved satisfactory and the unit was submitted to a full load/full speed test on the actual natural gas. Cluster limitations enabled maximum operation up to 23 MW at 5700 rpm with the unit in recycle mode—the test was passed flawlessly.

The torsional behavior of the unit was verified by means of a torque measuring device integrated in the coupling spacer. The measured first natural frequency is 27.5 Hz and has a low damping of about 1 percent. During normal operating conditions, only vibration with that first critical frequency occurred. Alternating torques during startup with low speed ramp reach their maximum of less than 15 percent of nominal torque at speeds of 2728, 2864, 3136, and 3272 rpm, coinciding with the resonance points of the Campbell diagram (Figure 17). Figure 29 shows a waterfall plot of the exciting torque pulsation in the air gap of the motor derived from measured electrical data during slow startup.

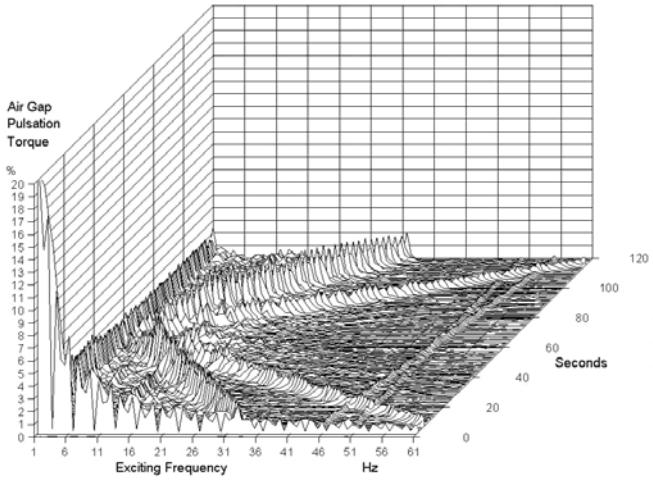

Figure 29. Measured Exciting Air Gap Torque Pulsation During Slow Startup.

The related mechanical torque pulsation in the main coupling is shown in Figure 30. Only the first torsional critical mode shape leads to significant amplifications. Measurement and calculation coincide as shown in Figures 31 and 32.

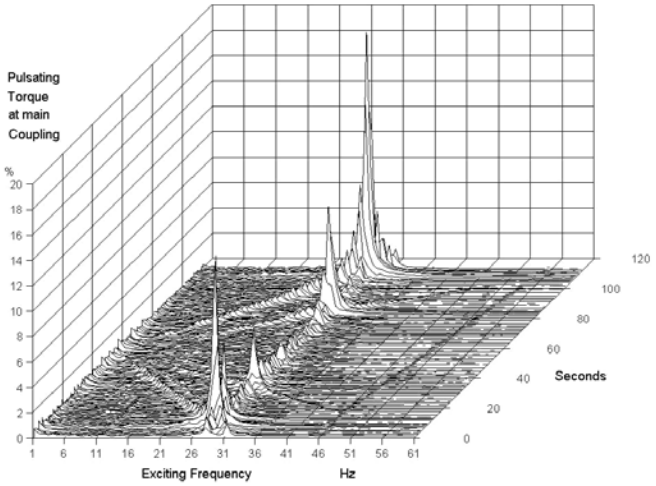

Figure 30. Measured Pulsating Torque Reaction at Main Coupling During Slow Startup.

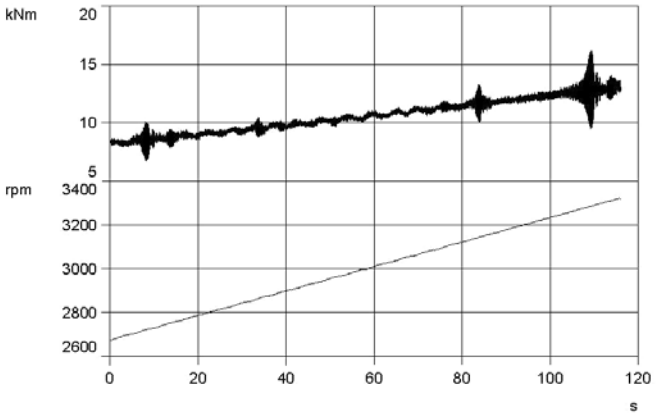

Figure 31. Measured Resonance Peaks near 3000 RPM.

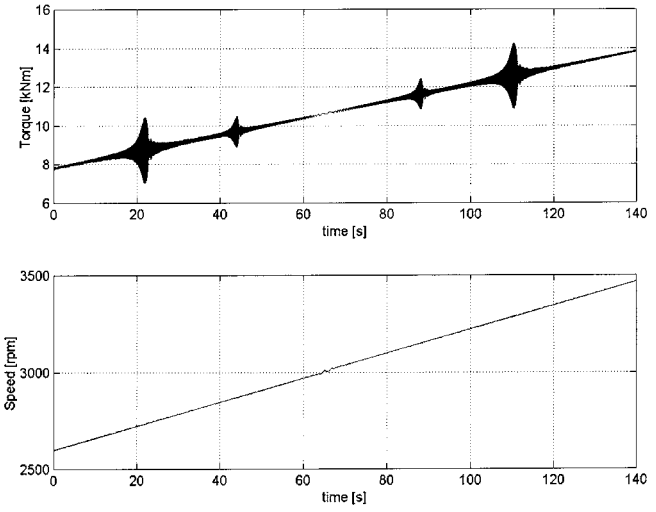

Figure 32. Calculated Resonance Peaks near 3000 RPM.

OPERATIONAL EXPERIENCE

The compression string has intermittently operated over its full speed and power range since November 1998. The total running time of the compressor as of the end of January 2000 is only about 800 hours, of which about 80 hours are at full load. This is due to limited operational demands. However, the standby hours of the plant, including rotor levitation and compressor under pressure, exceed 10,000 hours.

The only maintenance issue during this period has been the dry gas seals and the seal gas conditioning system. During site testing, several failures of the diaphragm type booster compressor occurred causing modifications to the seal gas system. This booster compressor is ensuring the supply of clean and dry seal gas for the low speed operating mode. Recall that minimum operation speed is as low as 10 percent. Once the modifications to the seal gas booster system had been implemented, performance was quite satisfactory with dry gas seals' leakage rates being consistently low on the order of 3 Nm^3/hr total. Field trials with and without the booster compressor in operation confirmed that the clean and dry Groningen gas conditions allow the elimination of the booster compressor from the system. As part of the generic design reassessment by the consortium, it was decided not to apply this booster compressor for the next unit that will be installed at the Bierum cluster.

Excessive gas leakage occurred after two months of operation, due to hangup of one of the dry gas seals. Field attempts to resolve this problem were not successful and the unit was shut down, the pullout pack removed, and shipped back to the manufacturer. The pullout pack was dismantled and the complete internals including the dry gas seals were covered with a fine corrosion dust. Various samples including field samples from the seal gas conditioning system were analyzed and it proved to be mainly rust coming from the 13 percent chromium (Cr) flow lines. The root cause for this rust was traced back to inadequate protection of these lines during site erection and commissioning, which resulted in prolonged exposure of the lines to the ambient air and hence the buildup of rust upstream of the compressor. During operation this rust found its way into the compressor and settled as a thin layer at the warmer internal parts of the compressor. Due to incorrect control logic, the antisurge valve inadvertently remained open during free flow operation of the installation. This caused wet gas to enter the compressor. This wet gas partly condensed and eventually filled the compressor with water that contained the corrosion dust. The water found its way deep into the dry gas seals and left a brown layer of dust at its internals. During operation, a dust dam built up, prohibiting free movement of the secondary seal element and resulting in a hangup of the dry gas seals. The pullout pack including the dry gas seals was cleaned and measures have been taken to prevent the hangup from reoccurring.

At the end of 1999, the unit was admitted to a three day endurance test under load. During this test, a close to 22 mln Nm^3/day flow rate was handled by the unit with suction conditions at 62 bara/30°C (899 psia/86°F) and discharge conditions ranging from 100 to 110 bara (1450 to 1595 psia) and 75 to 90°C (167 to 194°F). Power ranged from 15 to 20 MW and speed from 4500 to 5000 rpm. Operational restrictions not related to the unit prohibited full load/full speed operation. The unit passed this test flawlessly. Operating temperatures of the magnetic bearings stabilized at 100°C (212°F).

CONCLUSION AND LESSONS LEARNED

- The functional specification in combination with the TCoO evaluation methodology and the early forming of a cross-discipline manufacturer's team in a design competition did result in a better compression system concept with a significantly better overall efficiency and a wider operating envelope.
- The selection of the electric motor as prime mover has proven to be beneficial, particularly in view of the very wide continuous speed range, and the frequent remote start-stop operations.

- Annual natural gas savings are expected on the order of 14 mln Nm^3 per cluster compared with a traditional gas turbine solution.
- Absence of routine maintenance and consequential minimum human intervention on the compression string and low noise emissions allow for the omission of a compressor building, associated safety systems, and stationary cranes.
- The integrated design approach of compressor, motor, and bearing manufacturers is essential for such new developments and designs, particularly with an all magnetic bearing solution.
- Reliable operation of magnetic bearings throughout a very wide speed range including operation on lateral critical speeds has been proven.
- There still is a need to further simplify and improve dry gas seal systems. Initial field experience has shown that, by virtue of the clean and dry gas conditions at the compressor suction, the seal gas booster compressors can be eliminated on future joint venture installations.
- API should develop a comprehensive set of design guidelines and performance requirements for the use of magnetic bearings in high speed turbomachinery. This will ensure the correct application and take due account of the inherent benefits of magnetic bearings.

REFERENCES

API Standard 614, 1999, "Lubrication Shaft-Sealing and Control-Oil Systems for Special-Purpose Applications," American Petroleum Institute, Washington, D.C.

API Standard 617, 1995, "Centrifugal Compressors for Petroleum, Chemical, and Gas Service Industries," Sixth Edition, American Petroleum Institute, Washington, D.C.

ASME PTC-10, 1997, "Compressor and Exhausters," American Society of Mechanical Engineers, New York, New York.

ACKNOWLEDGEMENT

The authors wish to acknowledge the support and encouragement of the owners/operators of the subject installation, Nederlandse Aardolie Maatschappij B.V. (NAM), and the assistance and contributions of Dr. Günther Siegl and Hartmut Rauch, Siemens Dynamowerk Berlin; Fritz Kleiner, Siemens Oil & Gas Division Erlangen; and Viv Fletcher, Federal Mogul Magnetic Bearings, Shoreham-by-Sea, United Kingdom.